Journal of the Serbian Chemical Society
JSCS-info@shd.org.rs • www.shd.org.rs/JSCS
J. Serb. Chem. Soc. 79 (8) 1007–1017 (2014) UDC 546.623'21–31+542.913:66.017+539.24
JSCS–4643 *Original scientific paper*

Synthesis of micro–mesopores flower-like γ-Al_2O_3 nano-architectures

MOZAFFAR ABDOLLAHIFAR[1]*, MOHAMMAD REZA ZAMANI[2], EHSAN BEIYGIE[2] and HOSAIN NEKOUEI[3]

[1]*Department of Chemical Engineering, Science and Research Branch, Islamic Azad University, Kermanshah 67131, Iran,* [2]*Young Researchers' Club, Shahreza Branch, Islamic Azad University, Shahreza 86131, Iran and* [3]*Department of Industry, University of Applied Science and Technology, Larestan Branch, Larestan 74311, Iran*

(Received 3 September 2013, revised 20 January, accepted 21 January 2014)

Abstract: Micro–mesopores flowerlike γ-Al_2O_3 nano-architectures were synthesized by a thermal decomposition method using synthesized AlOOH (boehmite) as a precursor. After calcination at 500 °C for 5 h, the obtained flower-like γ-Al_2O_3 had a structure similar to that of the AlOOH precursor. X-Ray diffraction (XRD), FTIR, TG, FESEM and TEM techniques were used to characterize morphology and structure of the synthesized samples. The specific surface area (BET), pore volume and pore-size distribution of the products were determined by N_2 adsorption–desorption measurements. The flower-like γ-Al_2O_3 showed a high BET specific surface area of 148 m^2 g^{-1} with a total pore volume of 0.59 cm^3 g^{-1}.

Keywords: γ-Al_2O_3; micro–mesopores; nano-architecture; flower-like.

INTRODUCTION

Nowadays, materials, such as γ-Al_2O_3, having a crystalline framework, large porosity and high surface area are receiving a great deal of attention. Due to their thermal, chemical and mechanical stability, hydrated alumina or aluminum hydroxides find potential applications as ceramic oxides,[1] adsorbents,[2] catalysts,[3] catalyst supports[4] and are mainly used as refractory materials,[5] electrical insulators,[6] in electronics[7] and for ceramic membranes.[8] From another point of view, important usages requiring large tonnages of hydrated alumina or aluminum hydroxides are as fillers in polymer and plastics products and for the production of aluminum chemicals. Particularly, γ-Al_2O_3 is extensively used in catalysis or as an adsorbent due to its high porosity and surface area.[2,9] The alumina adsorbents and the catalytic performance of alumina-supported catalysts are, however,

* Corresponding author. E-mail: abdollahifar@gmail.com
doi: 10.2298/JSC130903007A

highly dependent on the textural and structural properties of the support and adsorbent, both of which depend on the synthesis procedure.

AlOOH is used as a precursor for γ-Al_2O_3, which is formed through the dehydration of the boehmite form of AlOOH at temperatures in the range 400––700 °C, whereby the produced γ-Al_2O_3 has the same morphology as that of the parent material.[10] Therefore, many efforts have been made to control the morphology of AlOOH. Hitherto, different morphologies of hierarchical AlOOH, such as microspheres consisting of nanosheets,[11] nanofibers,[12] nanotubes,[13] nanorods,[14] nanowires,[10] hollow nanospheres,[15] nano-belts,[16] cantaloupe-like architectures[17] and hollow and self-encapsulated microspheres[18] have been reported. Despite these previous extensive studies, the current knowledge concerning the formation of AlOOH structures of desired morphology for the production of γ-Al_2O_3 is still inadequate.

The hydrothermal route is one of the favorable and attractive methods for the synthesis of nanomaterials and nanostructures of very good quality. The products prepared *via* a hydrothermal route have good dispersity and crystallinity, and do not show macroscopic agglomeration. Moreover, the process conditions are moderate and easily controllable. The objective of the work reported herein, was to synthesize AlOOH by means of a hydrothermal treatment using aluminum nitrate and urea as the starting materials. A flower-like γ-Al_2O_3 nano-architecture was obtained by the thermal decomposition method using the synthesized AlOOH as the precursor.

EXPERIMENTAL

All the chemical materials used in the experiments were used without further purification. In a typical procedure, 18.75 g of $Al(NO_3)_3 \cdot 9H_2O$ (Scharlau, Spain, extra pure) and 6 g of urea, CH_4N_2O (Scharlau, Spain, synthesis grade) were dissolved in 100 and 30 mL of distilled water, respectively, at room temperature in beakers and magnetically stirred to obtain homogeneous solutions A and B, respectively. Then solution B was added to solution A and stirred at room temperature for 15 min before the mixed solution was transferred into a 200 mL Teflon-lined stainless autoclave and heated at 200 °C for several hours under autogenous pressure. After reaching room temperature, the precipitate was filtered, washed three times with distilled water, and finally dried in an oven at 60 °C for 24 h under air to afford a dried sample of boehmite. The flower-like γ-Al_2O_3 was prepared by dehydroxylation of the synthesized boehmite at 500 °C under air for 5 h. A schematic flow chart for the preparation of flower-like γ-Al_2O_3 is presented in Fig. 1.

Thermal analysis of the AlOOH sample was carried out on 10 mg powder sample under air up to 800 °C at a heating rate of 13 °C min^{-1} using a TG/DTA6300 (SII Nanotechnology, Japan) thermal analyzer that simultaneously provided thermogravimetric analysis (TG), derivative thermal analysis (DTG) and differential thermal analysis (DTA) curves. Fourier transform infrared spectroscopy (FTIR) was performed on RAYLEIGH, model WQF-510 instrument. X-Ray powder diffraction (XRD) analysis was conducted on a Bruker, model B8 Advance X-ray diffractometer with CuK_α radiation. The crystallite size of the particles of the samples were calculated using the Scherrer formula ($d = 0.9\lambda/(B\cos\theta)$, where d, λ, B, and θ are

the crystallite size, CuK_α wavelength (λ = 1.54 Å), full width at half-maximum intensity (FWHM) of the peak in radians and the Bragg diffraction angle, respectively). TEM images of the samples were taken using a PHILIPS model CM30 transmission electron microscope operated at an accelerating voltage of 250 kV. FESEM images were obtained using a HITACHI S-4160 field emission scanning electron microscope. The nitrogen adsorption and desorption isotherms at 77 K were measured using a BEL SORP, MINI II-310 adsorption analyzer after the samples had been degassed under vacuum at 200 °C for 3 h. The original Barrett, Joyner and Halenda (BJH) method[19] was applied for the calculation of the pore size distributions using the adsorption branch of the isotherms and the specific surface areas and pore volumes were determined by the BET method.

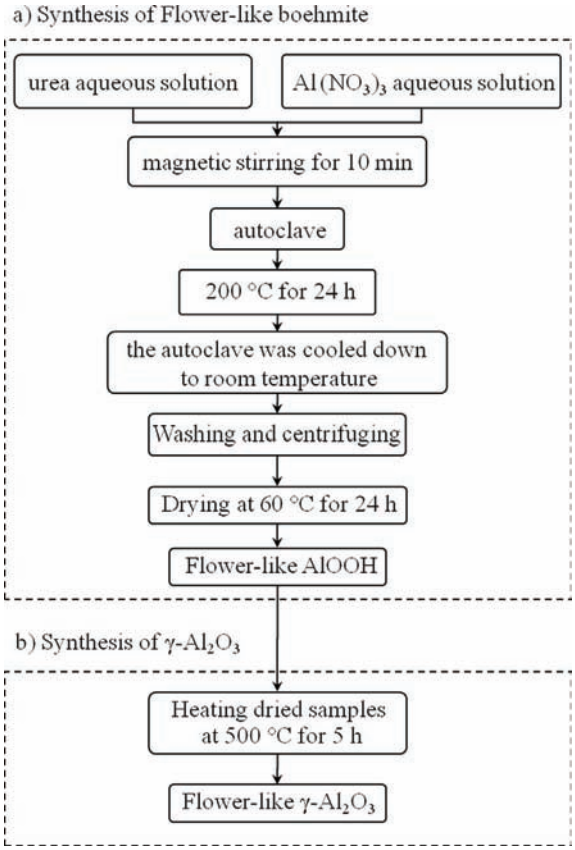

Fig. 1. Schematic flow chart for the preparation of a) AlOOH and b) γ-Al_2O_3.

RESULTS AND DISCUSSIONS

Figure 2 shows the XRD results of AlOOH and γ-Al_2O_3, Fig. 2a and b, respectively. The main diffraction peaks could be indexed within experimental error as the orthorhombic phase of boehmite AlOOH (JCPDS card No. 00-021--1307) and as cubic γ-Al_2O_3 (JCPDS card No. 00-001-1303), respectively. No

evidence could be found for the existence of impurities in the synthesized AlOOH and γ-Al_2O_3. The crystallite sizes calculated from the FWHM of the (120) diffractions for AlOOH and the (211) peaks for γ-Al_2O_3 using the Scherrer equation were found to be 12 and 10 nm, respectively.

Typical FT-IR spectra of the corresponding samples are shown in Fig. 3a and b. Figure 3a shows that all the absorption bands at 3300, 3096, 2098, 1638, 1518, 1390, 1156, 1066, 750, 640 and 492 cm^{-1} are consistent with the reported

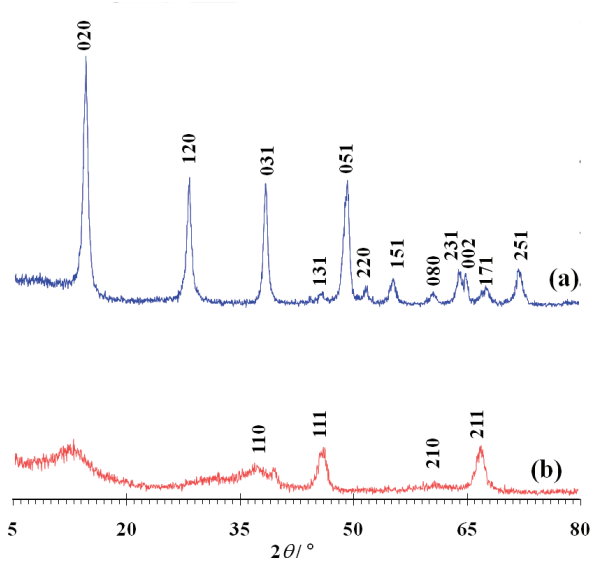

Fig. 2. XRD patterns of a) AlOOH and b) γ-Al_2O_3.

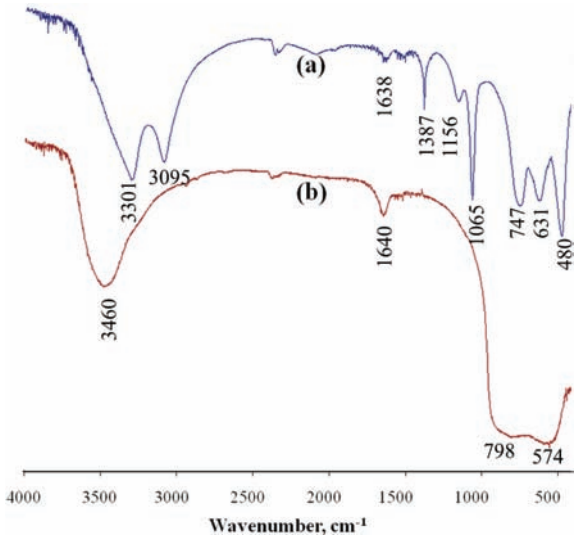

Fig. 3. FTIR spectrum of a) AlOOH and b) γ-Al_2O_3.

values for AlOOH,[20] which strongly support the formation of the synthesized sample. In the spectrum of the calcined powder shown in Fig. 3b, the peaks at 606 and 829 cm^{-1} are assigned to γ-AlO_6 and γ-AlO_4, respectively. Thus, the γ-Al_2O_3 phase contained both octahedral and tetrahedral coordination. The broad band at 3459 cm^{-1} and the weak band at 1641 cm^{-1} are due to adsorbed water.[21]

The temperature at which complete decomposition of organics had occurred can be determined by TG/DTA analysis. Thermal analysis data consisting of TG, DTG and DTA curves of the synthesized AlOOH are shown in Fig. 4. The chosen calcination temperature of 500 °C for the conversion of AlOOH into γ-Al_2O_3 was derived from the TG curve. The dehydration of AlOOH appears to occur in four steps. The first step, occurring in the temperature range 25–95 °C and accounting for 1.5 % of the estimated weight loss, may have been due to the loss of physisorbed water. The second step, occurring in the temperature range 95–230 °C with about 1.9 % weight loss, may be due to the loss of chemisorbed water. The third step with a mass loss of about 15.2 % occurred in the temperature range 230–500 °C, which could be ascribed to the conversion of AlOOH into

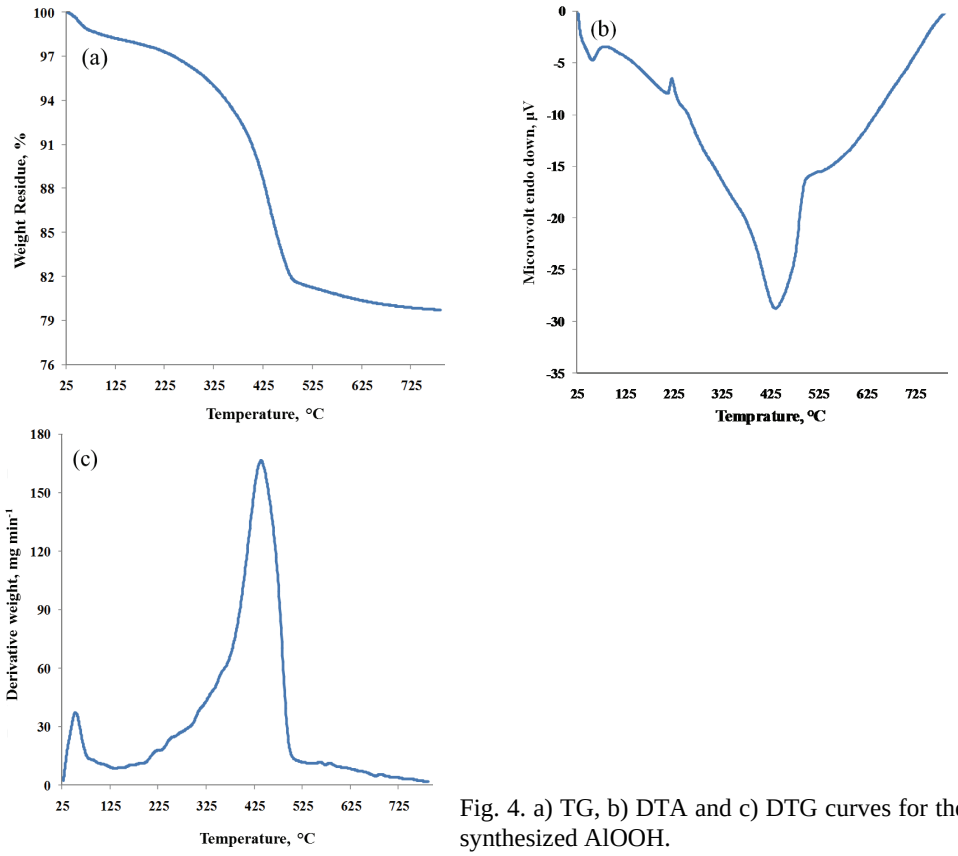

Fig. 4. a) TG, b) DTA and c) DTG curves for the synthesized AlOOH.

γ-Al_2O_3, while the weight loss (1.5 %) at temperatures above 500 °C is associated with the removal of the remaining hydroxyls. The weight losses appeared on the DTA curve as exothermic peaks that refer to several chemical processes, occurring because of thermal degradation of the synthesized AlOOH over the temperature ranges given in Table I.

TABLE I. Thermal data (TG, DTG and DTA) for the synthesized AlOOH; (–):exothermic

Temperature range, °C	DTG max. °C	Mass loss %	DTA °C	Assignment
25–95	54	1.5	58 (–)	Loss of physisorbed water
95–230	215	1.9	222 (–)	Loss of chemisorbed water
230–500	433	15.2	437 (–)	Conversion of alooh into γ-Al_2O_3
Above 500	–	1.5	–	Removal of remaining hydroxyls

The morphology and structure of the as-synthesized products were determined using FESEM and TEM. The FESEM images showing the flower-like nanostructures of AlOOH and γ-Al_2O_3 are presented in Fig. 5. The low-magnification images (Fig. 5a_1) shows that the AlOOH crystallites self-organize into flower-like assemblies. It can be seen from Fig. 5a_1 and b_1 that the morphology of AlOOH was retained after the formation of γ-Al_2O_3 by calcination. According to Fig. 5, several AlOOH and γ-Al_2O_3 nano-flowers appeared to be separate. To examine further the surface morphology of the flowerlike architectures, high--magnification FESEM images of both samples in the top view of the products,

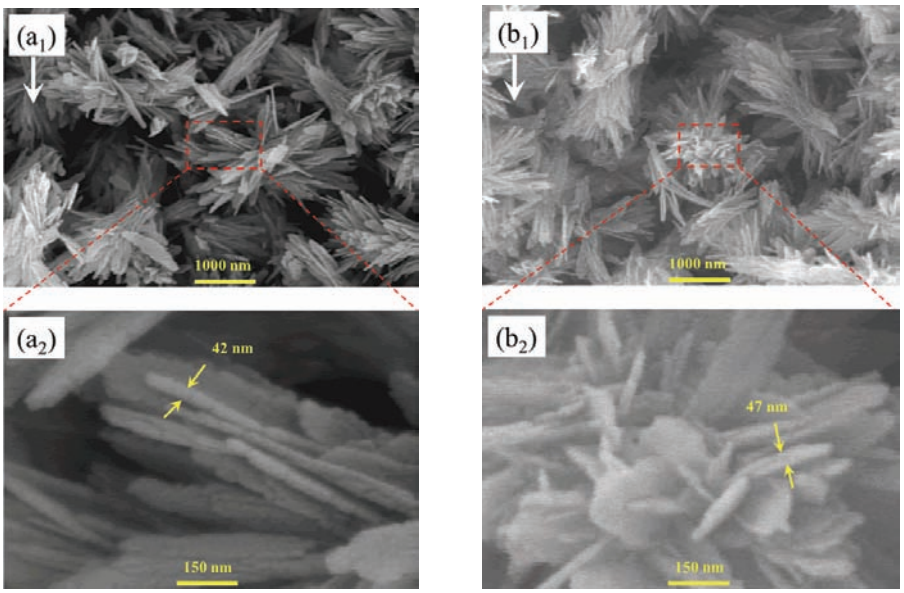

Fig. 5. FESEM images of the flower-like AlOOH (a_1 and a_2) and γ-Al_2O_3 (b_1 and b_2).

which were found to be constructed of several nano-pieces, were recorded, as shown in Figs. $5a_2$ and b_2.

The detailed structure of the γ-Al_2O_3 recorded as TEM micrographs is shown in Fig. 6. A low-magnification TEM image of γ-Al_2O_3 is shown in Fig. 6a and b; these might be detached parts from the flower-like nano-architectures or particles that aggregated in one-side flower structures. The nano-pieces were collected together by a center to form a hierarchical flower-like nanostructure. The high-magnification images of the nano-pieces structure of γ-Al_2O_3 could be observed clearly in Fig. 6e and f. In general, the FESEM micrographs are in good agreement with the TEM observations.

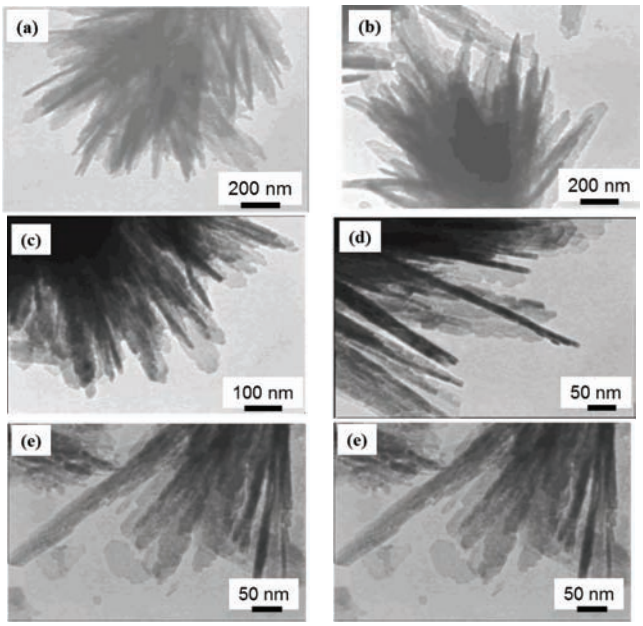

Fig. 6. TEM images of the fower-like γ-Al_2O_3.

The N_2 sorption isotherms of the synthesized AlOOH and γ-Al_2O_3 are illustrated in Fig. 7. The both samples showed a type IV isotherm with H1 + H3 type hysteresis loops, which indicated that these samples had some slit-shaped pores according to the Brunauer, Deming, Deming and Teller (BDDT) classification. This type of isotherm is characteristic for mesoporous samples. As could be seen from the adsorption and desorption curves, it was not a reversible phenomenon that led to the appearance of a hysteresis between the adsorption and desorption curves. The uptake of nitrogen by the both samples proceeded as monolayer–multilayer adsorption followed by capillary condensation, *i.e.*, instantaneous filling of mesopores with adsorbate, in the relative pressure (p/p_0) range of 0.90––0.99. However, the γ-Al_2O_3 showed a steep increase of the adsorption in the p/p_0

range 0.8–0.95, while the AlOOH displayed a gradual increase in the p/p_0 range 0.7–0.96, indicating that the γ-Al_2O_3 had larger mesopores than the AlOOH, as shown in the Table II. Thus, the formation of γ-Al_2O_3 resulted in a higher surface area and pore volume, but with a lower mean pore diameter. The inset of Fig. 7 presents the pore size distribution of the samples derived from the desorption branch of the N_2 adsorption/desorption isotherms. The pore size distribution curves for both samples showed one narrow and two wide distributions that were centered around 1.35, 12 and 26 nm, respectively. It can be seen that the intensity of peaks for the AlOOH were higher than those for γ-Al_2O_3.

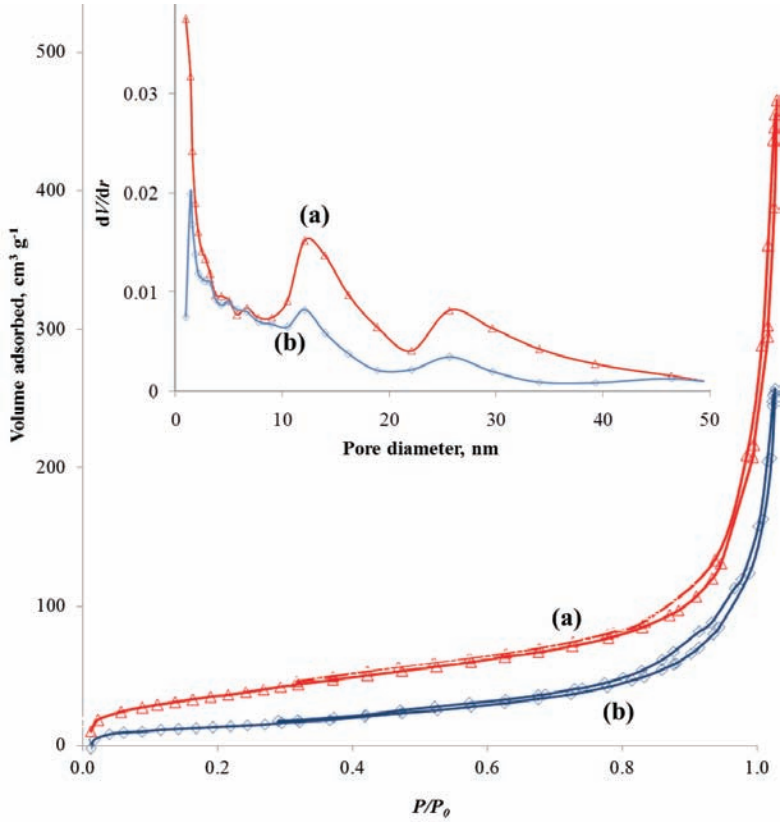

Fig. 7. Nitrogen adsorption/desorption isotherms and pore-size distribution (inset) of a) AlOOH and b) γ-Al_2O_3.

TABLE II. The textural properties of the samples

Sample	Surface area, $m^2\ g^{-1}$	Pore volume, $cm^3\ g^{-1}$	mean pore diameter, nm
AlOOH	69	0.36	21
γ-Al_2O_3	148	0.59	16

Further details concerning the structural characteristic of the synthesized AlOOH and γ-Al_2O_3, *i.e.*, the micropore volume in the presence of mesopores, are given in the *t*-plots presented in Fig. 8, from which, the contributions of the two different types of pores, namely micropores and mesopores, are obvious.

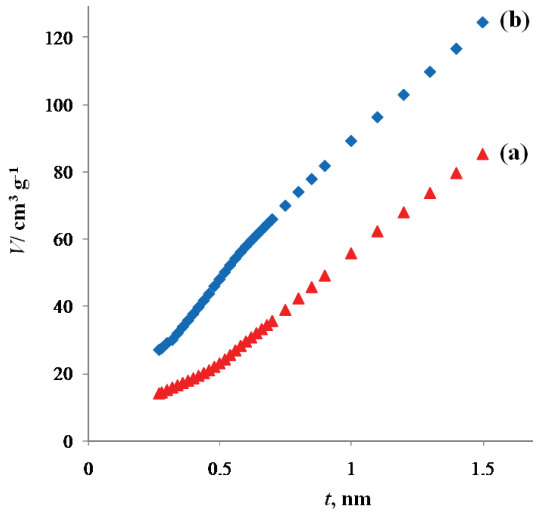

Fig. 8. *t*-Plot curves for a) AlOOH and b) γ-Al_2O_3.

In general, porous materials can contain more than one class of pores, *e.g.*, micropores and mesopores. It is possible to differentiate the contribution of micropores and mesopores to the surface area using the method developed by de Boer *et al.*[22] The nitrogen adsorption data can be plotted as a *t*-curve, in which the adsorbed nitrogen volume is presented as a function of the statistical thickness, *t*, of an adsorbed layer on a nonporous surface. If the adsorbent contains mesopores, capillary condensation occurs in each pore when the relative pressure reaches a value that is related to the pore radius by the Kelvin Equation, the *t*-plot therefore shows an upward deviation commencing at the relative pressure at which the finest pores are just being filled and the extrapolated plot passes through the origin. On the other hand, if microporosity exists, the uptake is enhanced in the low-pressure region and a positive intercept is observed that can be assigned to the micropore volume.

CONCLUSIONS

In summary, a micro/mesoporous flower-like γ-Al_2O_3 assembly from nano-pieces with a surface area of 148 m^2 g^{-1}, a mean pore diameter of 16 nm and a pore volume of 0.59 cm^3 g^{-1} was successfully synthesized by the decomposition of a synthesized AlOOH. The FESEM and TEM micrographs shows that the γ-Al_2O_3 was flower-like and a high-magnification micrograph of the sample showed that the products were constructed of several nano-pieces. The flower-

-like γ-Al_2O_3 is expected to have potential applications in catalysis, adsorption and other fields, due to its large surface area.

Acknowledgement. The support of the Islamic Azad University, Kermanshah Branch is greatly acknowledged.

ИЗВОД

СИНТЕЗА МИКРО–МЕЗОПОРОЗНОГ ЦВЕТАСТОГ γ-Al_2O_3 НАНОАРХИТЕКТУРЕ

MOZAFFAR ABDOLLAHIFAR[1], MOHAMMAD REZA ZAMANI[2], EHSAN BAYGI[2] и HOSAIN NEKOUEI[3]

[1]*Department of Chemical Engineering, Science and Research Branch, Islamic Azad University, Kermanshah 67131, Iran,* [2]*Young Researchers Club, Shahreza Branch, Islamic Azad University, Shahreza 86131, Iran и* [3]*Department of Industry, University of Applied Science and Technology, Larestan Branch, Larestan 74311, Iran*

Микро–мезопорозни наноструктурни γ-Al_2O_3 цветног облика добијен је методом термичке разградње синтетизованог AlOOH (бемит) као прекурсора. После калцинисања на температури 500 °C током 5 h, добијен је γ-Al_2O_3 облика цвета са структуром сличном AlOOH прекурсору. XRD, FTIR, TG, FESM и TEM технике коришћене су за карактерисање морфологије и структуре добијених узорака. Специфична површина (BET), запремина и расподела пора одредјиване су адсорпцијом/десорпцијом N_2. Цветаст γ-Al_2O_3 имао је велику специфичну површину- 148 $m^2\ g^{-1}$, са укупном запремином пора 0,59 $cm^3\ g^{-1}$.

(Примљено 23. септембра 2013, ревидирано 20. јануара, прихваћено 21. јануара 2014)

REFERENCES

1. S. A. Hassanzadeh Tabrizi, E. Taheri Nassaj, *Ceram. Int.* **37** (2011) 1251
2. Y. J. O. Asencios, M. R. Sun Kou, *Appl. Surf. Sci.* **258** (2012) 10002
3. A. M. D. A. Cruz, J. Guillaume Eon, *Appl. Catal., A* **167** (1998) 203
4. M. Fattahi, F. Khorasheh, S. Sahebdelfar, F. T. Zangeneh, K. Ganji, M. Saeedizad, *Sci. Iran.* **18** (2011) 1377
5. D. Larson, J. Coppola, D. Hasselman, R. Bradt, *J. Am. Ceram. Soc.* **57** (1974) 417
6. H. Bartzsch, D. Glob, B. Bocher, P. Frach, K. Goedicke, *Surf. Coat. Technol.* **174** (2003) 774
7. J. H. Choi, Y. M. Kim, Y. W. Park, T. H. Park, J. W. Jeong, H. J. Choi, E. H. Song, J. W. Lee, C. H. Kim, B. K. Ju, *Nanotechnology* **21** (2010) 475203
8. M. Moosemiller, C. Hill Jr., M. A. Anderson, *Sep. Sci. Technol.* **24** (1989) 641
9. P. P. Morajkar, J. B. Fernandes, *Catal. Commun.* **11** (2010) 414
10. J. Zhang, S. Wei, J. Lin, J. Luo, S. Liu, H. Song, E. Elawad, X. Ding, J. Gao, S. Qi, *J. Phys. Chem., B* **110** (2006) 21680
11. H. Liang, L. Liu, Z. Yang, Y. Yang, *Cryst. Res. Technol.* **45** (2010) 195
12. K. Mahmoodi, B. Alinejad, *Powder Technol.* **199** (2010) 289
13. L. Qu, C. He, Y. Yang, Y. He, Z. Liu, *Mater. Lett.* **59** (2005) 4034
14. X. Zhang, M. Honkanen, E. Levänen, T. Mäntylä, *J. Cryst. Growth* **310** (2008) 3674
15. D. H. M. Buchold, C. Feldmann, *Nano Lett.* **7** (2007) 3489
16. P. Gao, Y. Xie, Y. Chen, L. Ye, Q. Guo, *J. Cryst. Growth* **285** (2005) 555
17. Y. Feng, W. Lu, L. Zhang, X. Bao, B. Yue, Y. lv, X. Shang, *Cryst. Growth Des.* **8** (2008) 1426
18. W. Cai, J. Yu, S. Mann, *Microporous Mesoporous Mater.* **122** (2009) 42

19. E. P. Barrett, L. G. Joyner, P. P. Halenda, *J. Am. Chem. Soc.* **61** (1951) 373
20. W. Cai, J. Yu, S. Gu, M. Jaroniec, *Cryst. Growth Des.* **10** (2010) 3977
21. H. S. Potdar, K. W. Jun, J. W. Bae, S. M. Kim, Y. J. Lee, *Appl. Catal., A* **321** (2007) 109
22. J. H. de Boer, B. C. Lippens, B. G. Linsen, J. C. P. Broekhoff, A. van den Heuvel, T. J. Osinga, *J. Colloid Interface Sci.* **21** (1966) 405.